

Determination of the quadrupole moment of the 11^- isomer in ^{194}Pb via a double perturbation analysis of a level mixing spectroscopy measurement

K. Vyvey, D. Borremans, N. Coulier, R. Coussement, G. Georgiev, S. Teughels, and G. Neyens
Instituut voor Kern en Stralingsfysica, University of Leuven, Celestijnenlaan 200 D, B-3001 Leuven, Belgium

H. Hübel

Institut für Strahlen und Kern-physik, Universität Bonn, Nussallee 14-16, D-53115 Bonn, Germany

D. L. Balabanski

Faculty of Physics, St. Kliment Ohridsky University of Sofia, BG-1164 Sofia, Bulgaria

(Received 18 October 2001; published 25 January 2002)

The quadrupole moment of the 11^- isomer in ^{194}Pb has been determined as $|Q_s| = 4.48(86)e\text{ b}$ via a new extension of the level mixing spectroscopy technique (LEMS). The new analysis technique allows one to take into account the influence of the electric quadrupole and the magnetic dipole interactions of two subsequent isomers on the angular distribution of the lower lying γ -ray transitions. For each isomeric state the ratio of its quadrupole interaction frequency to its magnetic moment can be extracted from this double perturbation analysis, thus allowing to deduce their quadrupole moments provided that the electric field gradient and the magnetic moments are known.

DOI: 10.1103/PhysRevC.65.024320

PACS number(s): 23.20.En, 21.10.Ky, 27.80.+w

I. INTRODUCTION

Measurements of spectroscopic quadrupole moments provide a stringent test for nuclear models because these moments are related to the deformation of the nuclear states. Over the last decade several level mixing techniques have been developed for measuring quadrupole moments of a wide range of nuclear states [1–7]. One of the variants, the level mixing spectroscopy (LEMS) technique, is especially designed for measuring quadrupole moments of high spin isomers [6–10]. Several quadrupole moments of high spin isomers in the Pb region have already been measured by applying the LEMS technique [8,11]. A difficulty for the nuclei close to the $Z=82$ shell is, however, the cascades of isomers which are present. The angular distribution of the most intense low-lying γ -ray transitions depends on the electromagnetic interactions of all contributing isomers. A LEMS analysis, taking into account all electromagnetic perturbations of the preceding isomers, allows one to extract the ratio of the quadrupole interaction frequency to the magnetic moment of all these isomers. Hence, the quadrupole moments of the isomers can be deduced if the electric field gradient and the magnetic moments are known from other measurements. So far, LEMS is the only technique offering this possibility. Other techniques, such as the time-differential perturbed angular distribution (TDPAD) technique, fail when more than 1 isomer contributes to the angular distribution of the radiation. Note that a dedicated TDPAD analysis allows one to distinguish the g factors of subsequent isomers [12,13]. However, the analysis of a TDPAD quadrupole moment measurement is too complicated in the case of subsequent isomers because of the many frequencies superimposed in the time-differential spectrum [14].

The new LEMS analysis technique has been applied for the first time to extract the quadrupole moment of the 11^- isomer in ^{194}Pb , where both the decay of the 12^+ and the

11^- isomers are contributing to the intensity of the low lying γ ray transitions. The 11^- isomer in ^{194}Pb has the $\pi(s_{1/2}^{-2}h_{9/2}i_{13/2})$ proton configuration. Knowledge of its quadrupole moment allows to study the deformation of intruder states, which is discussed in Ref. [15]. Here, we deal with the experimental analysis procedure. Section II contains a theoretical study of the influence of the interaction of two subsequent isomers with the surrounding electromagnetic fields on the anisotropy of the γ radiation. In Sec. III the experimental results are presented. From the ratio of the deduced interaction frequencies for the 12^+ and the 11^- isomers the quadrupole moment of the 11^- isomer in ^{194}Pb is determined. The reliability of the new extension of the LEMS technique is demonstrated via the determination of the electric field gradient (EFG) of Pb in Re from the measured quadrupole interaction frequency of the $^{194}\text{Pb}(12^+)$ isomer.

II. EXPERIMENTAL METHOD

In order to discuss the influence of the electromagnetic interactions of two subsequent isomers on the anisotropy of the γ radiation as a function of the magnetic field strength, first the main principles of the LEMS formalism will be briefly repeated. More details about the LEMS technique can be found in Refs. [6,7].

A. The LEMS technique

In a LEMS experiment the electric quadrupole interaction is studied by implanting the isomer of interest in a crystal, providing the EFG, and applying an external magnetic field by means of a superconducting magnet. Either monocrystals or polycrystals can be used. In the case of a monocrystal the crystal is oriented such that the c -axis makes a large angle β ($\sim 40^\circ$) with the direction of the magnetic field.

In the axis system with the Z axis parallel to the direction of the magnetic field (lab system) the following nonvanishing matrix elements of the Hamiltonian $\mathcal{H}_{\text{LEMS}}$ are obtained for the combined magnetic dipole and electric quadrupole interaction [16]

$$\begin{aligned} \langle m | \mathcal{H}_{\text{LEMS}} | m \rangle \\ = -\hbar \omega_B m + \hbar \omega_Q \frac{1}{2} (3 \cos^2 \beta - 1) [3m^2 - I(I+1)], \end{aligned} \quad (1)$$

$$\begin{aligned} \langle m | \mathcal{H}_{\text{LEMS}} | m-1 \rangle \\ = -\frac{3}{2} \hbar \omega_Q \cos \beta \sin \beta (1-2m) \sqrt{(I-m+1)(I+m)}, \end{aligned} \quad (2)$$

$$\begin{aligned} \langle m | \mathcal{H}_{\text{LEMS}} | m-2 \rangle \\ = \frac{3}{4} \hbar \omega_Q \sin^2 \beta \\ \times \sqrt{(I+m-1)(I+m)(I-m+1)(I-m+2)}. \end{aligned} \quad (3)$$

Here $\omega_B = g\mu_N B/\hbar$ is the magnetic interaction frequency with g the gyromagnetic ratio, μ_N the nuclear magneton and B the magnetic field strength, $\omega_Q = eQ_s V_{ZZ}/\hbar 4I(2I-1)$ is the electric quadrupole frequency and Q_s is the spectroscopic quadrupole moment. It is assumed that the EFG is axially symmetric. The nondiagonal matrix elements, only present when the misalignment angle β differs from 0, cause a change of the orientation of the nuclear ensemble because they are responsible for a mixing of the different m states. When polycrystals are used the perturbation factors $G_{kk'}^{nn'}(I, \mathcal{H}_{\text{LEMS}}, \tau)$ (see below) need to be integrated over all possible angles β .

The change of the ensemble orientation of the oriented isomeric states with spin I is due to the applied electromagnetic interactions, governed by $\mathcal{H}_{\text{LEMS}}$. Via the detection of the angular distribution of the subsequent radiation the orientation change is measured as a function of the applied magnetic field. The perturbed angular distribution of the radiation is given by [17]

$$W(\theta, \phi, t) = \sqrt{4\pi} \sum_{k,n} \frac{1}{\sqrt{2k+1}} A_k U_k B_k^n(I, t) Y_k^n(\theta, \phi), \quad (4)$$

with A_k being the radiation parameters of the observed transitions, U_k describing the loss of orientation due to nondetected preceding γ rays, $B_k^n(I, t)$ being the perturbed orientation tensors at time t , and $Y_k^n(\theta, \phi)$ being the spherical harmonics in which θ and ϕ describe the detection directions with respect to the magnetic field direction. The orientation parameters at a certain time t are extracted from the initial orientation $B_k^n(I, t=0)$ parameters via [17]

$$B_k^n(I, t) = \sum_{k'n'} G_{kk'}^{nn'}(I, \mathcal{H}_{\text{LEMS}}, t) B_k^{n'}(I, t=0). \quad (5)$$

The initial orientation of the nuclear ensemble is created by the fusion-evaporation reaction itself and is axially symmetric around the beam axis. A Gaussian distribution with standard deviation σ is assumed [18]. The $G_{kk'}^{nn'}(I, \mathcal{H}_{\text{LEMS}}, t)$ are the perturbation factors that describe how the induced magnetic dipole and electric quadrupole interactions modify the relative population of the m -quantum states, as described by the density matrix ρ [17]. By using the direct relationship between the orientation tensors $B_k^n(I, t)$ and the matrix elements $\langle m' | \rho | m \rangle$ [19] and solving the time-evolution equation $i\hbar(d\rho/dt) = [\mathcal{H}_{\text{LEMS}}, \rho]$ the perturbation factors can be calculated explicitly as

$$G_{kk'}^{nn'}(I, \mathcal{H}_{\text{LEMS}}, t) = \sum_{NN'} (f_{NN'}^{\text{LEMS}})_{kk'}^{nn'} e^{-i\omega_{NN'}^{\text{LEMS}} t} \quad (6)$$

with

$$\begin{aligned} (f_{NN'}^{\text{LEMS}})_{kk'}^{nn'} &= \sqrt{2k+1} \sqrt{2k'+1} \sum_{m, \mu, N, N'} (-1)^{m-\mu} \\ &\times \begin{pmatrix} I & I & k \\ -m & m' & n \end{pmatrix} \begin{pmatrix} I & I & k' \\ -\mu & \mu' & n' \end{pmatrix} \langle m | N \rangle \\ &\times \langle N | \mu \rangle \langle m' | N' \rangle^* \langle N' | \mu' \rangle^* \end{aligned} \quad (7)$$

in which $\omega_{NN'} = (E_N - E_{N'})/\hbar$. E_N and $|N\rangle$ are the eigenvalues and eigenvectors of $\mathcal{H}_{\text{LEMS}}$. If the EFG is provided by a polycrystal and the magnetic field is oriented parallel to the beam axis only the $G_{kk'}^{00}$ terms need to be considered because of the axial symmetry of the system with respect to the symmetry axis of the initial orientation.

LEMS measurements are time-integrated measurements and, therefore, a time integration, taking into account the isomeric decay time τ , needs to be performed

$$G_{kk'}^{nn'}(I, \mathcal{H}_{\text{LEMS}}, \tau) = \frac{\int_0^\infty G_{kk'}^{nn'}(I, \mathcal{H}_{\text{LEMS}}, t) \exp(-t/\tau) dt}{\int_0^\infty \exp(-t/\tau) dt} \quad (8)$$

$$= \sum_{NN'} (f_{NN'}^{\text{LEMS}})_{kk'}^{nn'} \frac{1}{1 + i\omega_{NN'}^{\text{LEMS}} \tau}. \quad (9)$$

For $n=n'=0$ the real part equals

$$G_{kk'}^{00}(I, \mathcal{H}_{\text{LEMS}}, \tau) = \sum_{NN'} (f_{NN'}^{\text{LEMS}})_{kk'}^{00} \frac{1}{1 + (\omega_{NN'}^{\text{LEMS}} \tau)^2}, \quad (10)$$

while the imaginary part drops, because it is odd in $\omega_{NN'}^{\text{LEMS}}$.

The resulting LEMS curve is a decoupling curve, in which three regimes can be distinguished. At zero magnetic field only the electric quadrupole interaction is present and the initial orientation is reduced to the hard-core value. At

high magnetic fields (several T) the electric quadrupole interaction is negligible compared to the magnetic dipole interaction and the isomeric spins perform a Larmor precession around the magnetic field. If the magnetic field is oriented parallel to the beam axis, i.e., the axis of the initial orientation, the initial anisotropy induced by the nuclear reaction is measured. In between, there is competition between both interactions and a smooth change from the hardcore anisotropy to the initial full anisotropy is observed. This part of the LEMS curve is sensitive to the ratio of the quadrupole interaction frequency ν_Q to the magnetic moment μ . So, if the magnetic moment is known the quadrupole interaction frequency can be deduced.

Notice that a detectable perturbation of the orientation of the nuclear ensemble due to the electric quadrupole interaction is only possible if the lifetime of the isomeric state is long enough. This is the case if the lifetime τ , the quadrupole interaction frequency ν_Q , and the nuclear spin I , fulfill the LEMS condition

$$\nu_Q \tau / I > 0.5. \quad (11)$$

This condition is derived empirically in Ref. [20]. When the LEMS condition is fulfilled all $\omega_{NN'}^{\text{LEMS}}$ ($N \neq N'$) are large and give a negligible contribution in the time-integrated perturbation factor (10). The time-integrated perturbation factor is fully determined by the $N=N'$ terms and reduces to

$$G_{kk'}^{nn'}(I, \mathcal{H}_{\text{LEMS}}, \tau) = \sum_N (f_{NN}^{\text{LEMS}})^{nn'}. \quad (12)$$

B. Extension of the LEMS formalism towards two subsequent isomers interacting with electromagnetic fields

The high spin isomers of interest in a LEMS measurement are produced by a fusion-evaporation reaction. However, in a fusion-evaporation reaction many highly excited states are populated. They decay to the ground state by passing through a lot of intermediate states, some of them isomeric as well. All isomeric states having long enough life times (order of tens of nanoseconds) interact in a detectable way with the surrounding electromagnetic fields.

This subsection contains a theoretical description of the influence of the electromagnetic interactions on the angular distribution of the γ rays if two isomeric levels, each of them having a corresponding ratio ν_Q/μ , are present in the decay path. In principle, a further expansion towards interactions with more isomers is possible. However, in practice the analysis for more than two subsequent perturbations is complicated due to the many parameters involved. Therefore, the theoretical description is restricted to two contributing isomers.

1. The perturbation factor for two subsequent perturbations

Assume two isomers 1 and 2, having the nuclear properties $(I_1, \tau_1, Q_1, \mu_1)$ and $(I_2, \tau_2, Q_2, \mu_2)$, respectively. Isomer 1 is populated directly in the nuclear reaction or from higher levels by prompt γ decay. It decays after a time $t=t_1$ via a cascade of prompt γ rays to isomer 2. t_1 can be any time in

the time interval $[0, \infty]$, however with a probability which is quantified by $\exp(-t_1/\tau_1)$, in which τ_1 is the nuclear life time of isomer 1. The initial orientation of the isomeric state 1 is given by $B_k^n(I_1, t=0)$. This orientation is perturbed due to the interaction of the nuclear moments μ_1 and $Q_{s,1}$ with the surrounding electromagnetic fields. At the moment of decay, t_1 , the orientation can be written as [6]

$$B_{k_1}^{n_1}(I_1, t=t_1) = \sum_{k,n} G_{k_1 k}^{n_1 n}(I_1, \mathcal{H}_{\text{LEMS1}}, t_1) B_k^n(I_1, t=0). \quad (13)$$

The initial orientation of isomer 2 equals the final orientation of isomer 1 corrected by the deorientation coefficients $U_{k_1}(R_1)$ which take into account the loss of orientation due to the intermediate prompt γ rays. Therefore, the initial orientation of isomer 2 is given by

$$\begin{aligned} B_{k_1}^{n_1}(I_2, t=t_1) &= U_{k_1}(R_1) B_{k_1}^{n_1}(I_1, t=t_1) \\ &= U_{k_1}(R_1) \sum_{k,n} G_{k_1 k}^{n_1 n}(I_1, \mathcal{H}_{\text{LEMS1}}, t_1) \\ &\quad \times B_k^n(I_1, t=0). \end{aligned} \quad (14)$$

Isomer 2 interacts with the electromagnetic fields during the time interval $[t_1, t_2]$. At the time $t=t_2$ ($t_2 \in [t_1, \infty]$), also isomer 2 decays with a weighted probability $\exp[-(t-t_1)/\tau_2]$, in which τ_2 is the nuclear lifetime of isomer 2. Its orientation at the moment of decay, t_2 , is

$$\begin{aligned} B_{k_2}^{n_2}(I_2, t=t_2) &= \sum_{k_1, n_1} G_{k_2 k_1}^{n_2 n_1}(I_2, \mathcal{H}_{\text{LEMS2}}, t_2 - t_1) B_{k_1}^{n_1}(I_2, t=t_1) \\ &= \sum_{k_1, n_1} G_{k_2 k_1}^{n_2 n_1}(I_2, \mathcal{H}_{\text{LEMS2}}, t_2 - t_1) U_{k_1}(R_1) \\ &\quad \times \sum_{k,n} G_{k_1 k}^{n_1 n}(I_1, \mathcal{H}_{\text{LEMS1}}, t_1) B_k^n(I_1, t=0) \\ &= \sum_{k,n} G_{k_2 k}^{n_2 n}(I_1, I_2, \mathcal{H}_{\text{LEMS1}}, \mathcal{H}_{\text{LEMS2}}, t) \\ &\quad \times B_k^n(I_1, t=0). \end{aligned} \quad (15)$$

After the decay of isomer 2 no further change of the orientation takes place. Hence, the perturbation factor for two subsequent perturbations at a time $t > t_2$ is

$$\begin{aligned} &G_{k_2 k}^{n_2 n}(I_1, I_2, \mathcal{H}_{\text{LEMS1}}, \mathcal{H}_{\text{LEMS2}}, t) \\ &= \sum_{k_1, n_1} G_{k_2 k_1}^{n_2 n_1}(I_2, \mathcal{H}_{\text{LEMS2}}, t_2 \\ &\quad - t_1) U_{k_1}(R_1) G_{k_1 k}^{n_1 n}(I_1, \mathcal{H}_{\text{LEMS1}}, t_1). \end{aligned} \quad (16)$$

The following expression for the time-integrated perturbation factor is then obtained:

$$G_{k_2k}^{n_2n}(I_1, I_2, \mathcal{H}_{\text{LEMS1}}, \mathcal{H}_{\text{LEMS2}}, \tau_1, \tau_2) = \sum_{N_1, N'_1, N_2, N'_2, k_1, n_1} (f_{N_2 N'_2}^{\text{LEMS2}})_{k_2 k_1}^{n_2 n_1} U_{k_1}(R_1) (f_{N_1 N'_1}^{\text{LEMS1}})_{k_1 k}^{n_1 n} \times \frac{\int_0^\infty \exp(-t_1/\tau_1) \exp(-i\omega_{N_1 N'_1}^{\text{LEMS1}} t_1) \int_{t_1}^\infty \exp[-(t-t_1)/\tau_2] \exp[-i\omega_{N_2 N'_2}^{\text{LEMS2}} (t-t_1)] dt dt_1}{\int_0^\infty \exp(-t_1/\tau_1) \int_{t_1}^\infty \exp[-(t-t_1)/\tau_2] dt dt_1}. \quad (17)$$

The integrals can easily be calculated in an analytical way:

$$\begin{aligned} G_{k_2k}^{n_2n}(I_1, I_2, \mathcal{H}_{\text{LEMS1}}, \mathcal{H}_{\text{LEMS2}}, \tau_1, \tau_2) &= \sum_{N_1, N'_1, N_2, N'_2, k_1, n_1} (f_{N_2 N'_2}^{\text{LEMS2}})_{k_2 k_1}^{n_2 n_1} U_{k_1}(R_1) \\ &\times (f_{N_1 N'_1}^{\text{LEMS1}})_{k_1 k}^{n_1 n} \left(\frac{1}{1 + i\omega_{N_1 N'_1}^{\text{LEMS1}} \tau_1 + i\omega_{N_2 N'_2}^{\text{LEMS2}} \tau_1} \right) \\ &\times \left(\frac{1}{1 + i\omega_{N_2 N'_2}^{\text{LEMS2}} \tau_2} \right). \end{aligned} \quad (18)$$

The time-integrated double perturbation factor is NOT equal to the product of the two time-integrated single perturbation factors times the deorientation coefficient $G_{k_1 k}^{n_1 n}(I_1, \nu_{Q_1}/\mu_1, \tau_1) U_{k_1}(R_1) G_{k_2 k_1}^{n_2 n_1}(I_2, \nu_{Q_2}/\mu_2, \tau_2)$, because an extra $i\omega_{N_2 N'_2}^{\text{LEMS2}} \tau_1$ term is present in the denominator. However, if the LEMS condition (11) for isomer 2 is fulfilled, then similar to Eq. (12) only the $\omega_{N_2 N'_2}^{\text{LEMS2}} (N_2=N'_2) = 0$ terms contribute and the formula reduces to

$$\begin{aligned} G_{k_2k}^{n_2n} \left(I_1, I_2, \frac{\nu_{Q_1}}{\mu_1}, \frac{\nu_{Q_2}}{\mu_2}, \tau_1, \tau_2 \right) &= G_{k_1 k}^{n_1 n} \left(I_1, \frac{\nu_{Q_1}}{\mu_1}, \tau_1 \right) U_{k_1}(R_1) G_{k_2 k_1}^{n_2 n_1} \left(I_2, \frac{\nu_{Q_2}}{\mu_2}, \tau_2 \right). \end{aligned} \quad (19)$$

2. The influence of the other decay branches on the angular distribution function

In the most general case a γ ray in the cascade below isomer 2 contains 4 contributions (Fig. 1): A first fraction $D1$ originates directly from isomer 1, bypassing isomer 2 in its decay. Further, a certain fraction $D2$ of the isomers 2 is not fed via isomer 1, but directly by a cascade of prompt γ rays, which are either discrete or statistical. We will refer to this as ‘‘direct feeding.’’ Obviously, also a double perturbed fraction $2P$ is present. Finally, side feeding into levels below isomer 2 ensures a prompt component as well. In practice reliable fit results are obtained by neglecting the prompt component (which does not influence the extracted frequency ν_Q), thus rescaling the fractions $D1, D2$ and $2P$ such that $D1 + D2$

+ $2P = 100\%$. Hence, the time-integrated angular distribution function for R contains three contributions

$$\begin{aligned} W(\theta, \phi) &= W(\theta, \phi, D1) D1 + W(\theta, \phi, D2) D2 \\ &+ W(\theta, \phi, 2P) 2P. \end{aligned} \quad (20)$$

Here

$$\begin{aligned} W(\theta, \phi, D1) &= \sqrt{4\pi} \sum_{k_2 \text{ even}} \frac{1}{\sqrt{2k_2 + 1}} A_{k_2}(\gamma) Y_{k_2}^{n_2}(\theta, \phi) U_{k_2}(R'_1) \\ &\times G_{k_2 k}^{n_2 n}(I_1, \mathcal{H}_{\text{LEMS1}}, \tau_1) B_k^n(I_1, t=0) \end{aligned} \quad (21)$$

is the contribution due to the perturbation of isomer 1. The contribution due to the single perturbation of isomer 2 is

$$\begin{aligned} W(\theta, \phi, D2) &= \sqrt{4\pi} \sum_{k_2 \text{ even}} \frac{1}{\sqrt{2k_2 + 1}} A_{k_2}(\gamma) Y_{k_2}^{n_2}(\theta, \phi) U_{k_2}(R_2) \\ &\times G_{k_2 k}^{n_2 n}(I_2, \mathcal{H}_{\text{LEMS2}}, \tau_2) B_k^n(I_2, t=0) \end{aligned} \quad (22)$$

and the contribution due to the double perturbation of isomer 2 is

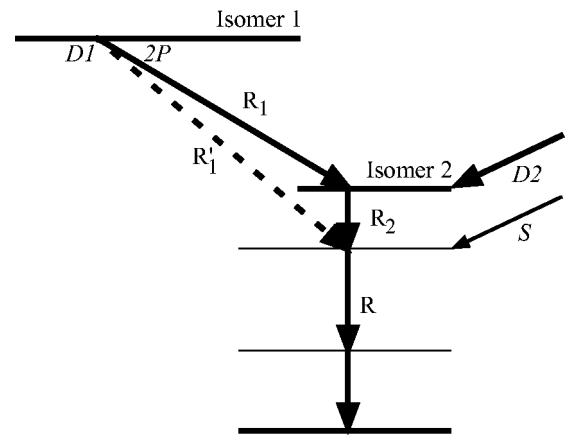
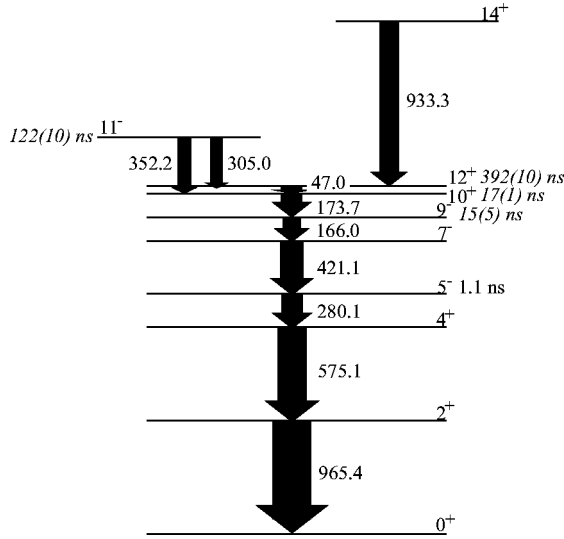


FIG. 1. Decay scheme of a nucleus in which two isomers are present. The labels $D1$, $D2$, $2P$, and S denote the direct feeding (see text) via isomer 1, the direct feeding via isomer 2, the double perturbed fraction, and the side feeding, respectively. The γ rays of interest are labeled R_1 , R_2 , R'_1 , and R .


 FIG. 2. Partial level scheme of ^{194}Pb (taken from Ref. [23]).

$$\begin{aligned}
 W(\theta, \phi, 2P) = & \sqrt{4\pi} \sum_{k_{\text{even}}} \frac{1}{\sqrt{2k_2+1}} A_{k_2}(\gamma) Y_{k_2}^{n_2}(\theta, \phi) U_{k_2}(R_2) \\
 & \times G_{k_2 k}^{n_2 n}(I_1, I_2, \mathcal{H}_{\text{LEMS1}}, \mathcal{H}_{\text{LEMS2}}, \tau_1, \tau_2) \\
 & \times B_k^n(I_1, t=0). \quad (23)
 \end{aligned}$$

The analysis of a double perturbed decay implies seven parameters: the direct feedings $D1$ and $D2$, the initial orientations for both isomers $(\sigma/I)_1$ and $(\sigma/I)_2$, the ratios of the nuclear moments for each isomer, $(\nu_Q/\mu)_1$ and $(\nu_Q/\mu)_2$, and a normalization factor N , depending on the detector efficiencies. The fractions of the direct feedings $D1$ and $D2$, can be determined from the relative intensities of the γ rays R_1, R'_1, R_2 , and R (see Fig. 1) so that only five parameters remain.

III. EXPERIMENTAL RESULTS

The technique has been applied to extract the quadrupole interaction frequencies of the 11^- and 12^+ isomers in ^{194}Pb implanted in a Re host. The $50 \mu\text{m}$ thick ^{nat}Re foil served as a target, a LEMS host and a beam stopper at the same time.

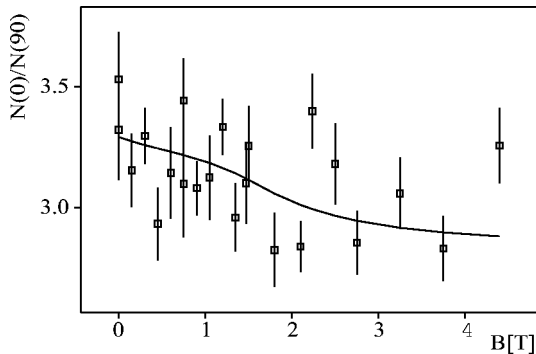
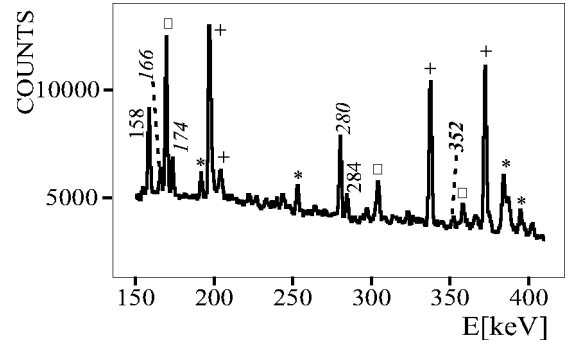

 FIG. 3. LEMS curve for the 352 keV transition depopulating the $^{194}\text{Pb}(11^-)$ isomer. The fit results in $\nu_Q = 280_{-200}^{+270}$ MHz.


FIG. 4. A typical spectrum obtained in the $^{nat}\text{Re}(^{14}\text{N}, xn)$ reaction at a beam energy of 87 MeV after 15 min of measurement time. The peaks originating from the $^{194}\text{Pb}(12^+)$ and $^{194}\text{Pb}(11^-)$ isomers are indicated in italic and bold-italic font, respectively. The energies of the peaks due to Coulomb excitation on ^{nat}Re are in normal font. Contaminating radiation, which is either prompt or from other isomers or from β decay, is marked with a square, a cross and an asterisk, respectively.

^{nat}Re has an hcp lattice structure and consists of 62.6% ^{187}Re and 37.4% ^{185}Re [21]. The ^{14}N beam with an energy of 87 MeV was delivered by the CYCLONE cyclotron at Louvain-la-Neuve. The data were taken at room temperature. Typically 16 spectra of 15 min. were collected at each magnetic field. No beam pulsing was used. One Ge detector was positioned parallel to the magnetic field, while two other detectors, one of which was a planar detector, were positioned at 90° with respect to the magnetic field. In order to account for unphysical effects due to beam fluctuations, etc., an extra normalization of all data points with the prompt 158 keV transition, present due to Coulomb excitation on ^{185}Re [22], has been performed.

The analysis of the 352 keV $E1$ transition, directly depopulating the 11^- isomer (Fig. 2 and Ref. [23]), resulted in a huge experimental uncertainty $\nu_Q = 280_{-200}^{+270}$ MHz (Fig. 3). This is due to the low intensity of the transition and the presence of contaminating radiation (Fig. 4). Therefore, the 965 keV ($E2$), 575 keV ($E2$), 280 keV ($E1$), and 166 keV ($E2$) transitions in the cascade underneath the 12^+ isomer have been analyzed and a double perturbation fit has been performed. The magnetic moment of the 12^+ isomer has been measured as $\mu = 2.004(24) \mu_N$ [24]. No experimental data on the magnetic moment of the 11^- isomer were available and, therefore, the experimentally deduced magnetic moment of the 11^- isomer in ^{196}Pb , $\mu_N = -1.920(18) \mu_N$, has been adopted [25]. This choice is justified as both the 11^- isomers in ^{194}Pb and ^{196}Pb have the same $\pi(s_{1/2}^{-2} i_{13/2} h_{9/2})$ configuration and the magnetic moments of the 11^- isomers in the even Po isotopes, having the $\pi(i_{13/2} h_{9/2})$ proton configuration, are shown to be little mass dependent [26]. Apart from the two quadrupole interaction frequencies also the the amount of initial orientation σ/I of the 12^+ isomer and a normalization factor N have been taken as free fit parameters. The initial orientation of the 11^- isomer was kept equal to the initial orientation of the 12^+ isomer [$\sigma/I(11^-) = \sigma/I(12^+)$] in order to eliminate one more free fit parameter. This is a reasonable assumption because

TABLE I. Experimental results obtained for the transitions depopulating the $^{194}\text{Pb}(11^- \rightarrow 12^+)$ cascade. The right column contains the values for $\nu_Q(12^+)$ obtained from a fit supposing that only the 12^+ isomer contributes to the perturbation of the angular distributions.

E_γ (keV)	Detector ratio	$\nu_Q(12^+)$ (MHz)	$\nu_Q(11^-)$ (MHz)	$\nu_Q(12^+)$ (MHz)
166	1	30_{-5}^{+7}	285_{-80}^{+120}	37.5(6.0)
166	2	37_{-5}^{+6}	340(70)	48(5)
280	1	$23.5_{-5.5}^{+10.5}$	190_{-90}^{+40}	29(3)
280	2	22.5(4)	220_{-40}^{+60}	30(4)
575	1	27(4)	330_{-60}^{+140}	39(6)
965	1	30(4)	290(40)	41(6)
weighted mean		28(2)	262(41)	36.0(2.5)

both isomers were produced in the same reaction and have a similar excitation energy and spin. The direct feedings of the isomers D_{11^-} and D_{12^+} have been determined from the relative γ ray intensities of the 173, the 352, 305, and 933 keV transitions. As the 352 and 305 keV transitions could not be analyzed in a reliable way from our data, the relative intensities were adopted from Refs. [27,23], where the $^{188}\text{Os}(^{12}\text{C},6n)$, $^{162}\text{Dy}(^{36}\text{S},4n)$, and $^{150}\text{Sm}(^{48}\text{Ca},4n)$ reactions were used. Rescaling the fractions such that $D_{11^-} + D_{12^+} + 2P_{11^- \rightarrow 12^+} = 100\%$ finally results in $D_{11^-} = 25\%$, $D_{12^+} = 60\%$ and $2P_{11^- \rightarrow 12^+} = 15\%$. The half-lives of the 10^+ level [$T_{1/2} = 17(1)$ ns], the 9^- level [$T_{1/2} = 15(5)$ ns], and the 5^- level ($T_{1/2} = 1.1$ ns) are too short for detectable electromagnetic interactions (the anisotropy at a magnetic field $B=0$ T differs less than 0.2% from the anisotropy of the initial orientation). Therefore, in the fit these levels are considered to be prompt.

The fits resulted in the quadrupole interaction frequencies $\nu_Q(^{194}\text{Pb}; I^\pi = 12^+) = 28(2)$ MHz and $\nu_Q(^{194}\text{Pb}; I^\pi = 11^-) = 262(41)$ MHz, respectively. The experimental uncertainties include the uncertainty of the magnetic moment as well as the uncertainties due to the fixing of some parameters as described above. The values are the average of the results obtained from several transitions and different detector combinations as listed in Table I. Sample LEMS curves are shown in Fig. 5.

Prior to our experiments the quadrupole moment of the $^{194}\text{Pb}[I^\pi = 12^+, T_{1/2} = 392(10)\text{ns}, \mu = 2.004(24)\mu_N]$ has been measured as $Q_s = 0.49(3)e b$ by applying the TDPAD technique [24]. Hence, the EFG of Pb in Re could be deduced from the frequency $\nu_Q(^{194}\text{Pb}; I^\pi = 12^+)$ as $|V_{ZZ}| = 2.36(23) \times 10^{21}$ V/m². This value is in perfect agreement with the value of $|V_{ZZ}| = 2.42(27) \times 10^{21}$ V/m², which was derived from the quadrupole interaction frequency of the $^{196}\text{Pb}(I^\pi = 12^+)$ isomer implanted in the same Re host [28]. For comparison, Table I also lists the quadrupole interaction frequencies derived from a fit assuming that the $^{194}\text{Pb}(11^-)$ isomer does not contribute to the 166, 280, 575, and 965 keV γ ray intensities. They result in a frequency $\nu_Q = 36.0(2.5)$ MHz and $|V_{ZZ}| = 3.04(28) \times 10^{21}$ V/m². This value is too high compared to the value obtained from the

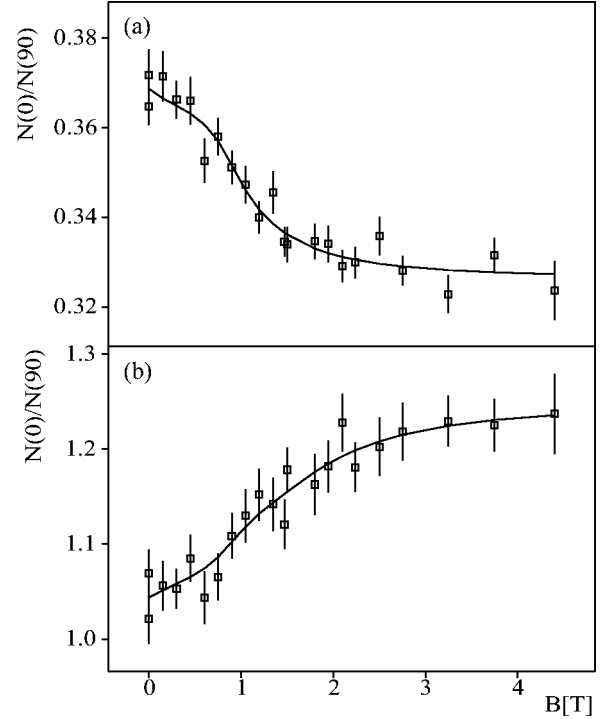


FIG. 5. Sample LEMS curves for the transitions depopulating the $^{194}\text{Pb}(12^+)$ cascade. The data are normalized on the prompt 158 keV transition in ^{185}Re . (a) LEMS curve for the 280 keV $E1$ transition. (b) LEMS curve for the 166 keV $E2$ transition. The fit results are listed in Table I.

quadrupole interaction frequency of the $^{196}\text{Pb}(I^\pi = 12^+)$ isomer. Hence, these results prove the reliability of the double perturbation formalism. In principle, the double perturbation formalism needs to be applied as well for the analysis of the 337 keV transition depopulating the 12^+ isomer in ^{196}Pb , as published in Ref. [28]. Indeed, also this transition contains a contribution due to the presence of the 11^- isomer on top of it. However, because the ratio ν_Q/μ is almost identical for the 11^- and the 12^+ isomers in ^{196}Pb [$(\nu_Q/\mu; 11^-) = 19(3)$ MHz/ μ_N and $(\nu_Q/\mu; 12^+) = 18(2)$ MHz/ μ_N] the simple LEMS analysis and the analysis taking into account the double perturbations give rise to the same result $\nu_Q(^{196}\text{Pb}; 12^+) = 38(3)$ MHz.

The quadrupole moment of the $^{196}\text{Pb}(12^+)$ isomer was measured before as $Q_s = 0.65 e b$ [29]. Therefore, the quadrupole moment of the $^{194}\text{Pb}(11^-)$ isomer could be deduced from the ratio of the quadrupole interaction frequencies $\nu_Q(^{194}\text{Pb}; 11^-)/\nu_Q(^{196}\text{Pb}; 12^+)$, as $|Q_s(^{194}\text{Pb}; 11^-)| = 4.48(86)e b$. From the measured spectroscopic quadrupole moment we derive the isomeric deformation as $|\beta_2| = 0.21(4)$ by applying the standard formulas $Q_s = Q_0[3K^2 - I(I+1)]/[(I+1)(2I+1)]$ and $Q_0 = (3/\sqrt{5}\pi)R_0^2 Z\beta_2(1 + 0.36\beta_2)$ [30]. Hence, we can conclude from the experimental result that the 11^- isomer in ^{194}Pb is a deformed nuclear state, in agreement with earlier theoretical calculations predicting a moderately oblate deformation [31]. The significance of this nuclear physics result is extensively discussed in Ref. [15].

IV. CONCLUSION

In this paper we have extracted the quadrupole moment of the 11^- isomer in ^{194}Pb as $|Q_s| = 4.48(86)e$ b by applying a double perturbation analysis of LEMS data for the first time. This extension to the analysis procedure allows to extract the ratios of the quadrupole interaction frequencies to the magnetic moments for all isomers which contribute to the intensity of a certain γ ray transition. The reliability of the technique has been proven by extracting the EFG of Pb in Re. The value obtained from this work for the EFG of ^{194}Pb in Re, $|V_{ZZ}(\text{PbRe})| = 2.36(23) \times 10^{21}$ V/m² is in perfect agreement with the value obtained in Ref. [28]. The obtained quadrupole moment for the 11^- isomer in ^{194}Pb corresponds to a deformation $\beta_2 = 0.21(4)$. This confirms former calcu-

lations, yielding a moderately deformed oblate shape for intruder isomers in this neutron-deficient Pb region [31].

ACKNOWLEDGMENTS

The authors are grateful to the engineers of the CYCLONE cyclotron, Louvain-la-Neuve, Belgium, for providing the excellent beam. This work is partially financed by the IUAP Project No. p4-07, with a grant for G.G. G.N. acknowledges support of the Flemish Science Foundation (FWO-Vlaanderen). D.L.B. is supported in part by the Bulgarian National Science Fund. The authors also acknowledge support through the EU TMR/LFS Contract No. ERB FMG ECT 950026.

-
- [1] G. Scheveneels, F. Hardeman, G. Neyens, and R. Coussement, *Hyperfine Interact.* **52**, 257 (1989).
- [2] G. Neyens, R. Nouwen, and R. Coussement, *Nucl. Instrum. Methods Phys. Res. A* **340**, 555 (1994).
- [3] G. Neyens, N. Coulier, S. Ternier, K. Vyvey, S. Michiels, R. Coussement, D.L. Balabanski, J.M. Casandijan, M. Chartier, D. Cortina-Gil, M. Lewitowicz, W. Mittig, A.N. Ostrowski, P. Roussel-Chomaz, N. Alamanos, and A. Lépine-Szilý, *Phys. Lett. B* **393**, 36 (1997).
- [4] G. Neyens, N. Coulier, S. Teughels, G. Georgiev, B.A. Brown, W.F. Rogers, D.L. Balabanski, R. Coussement, A. Lépine-Szilý, M. Lewitowicz, W. Mittig, F. de Oliveira Santos, P. Roussel-Chomaz, S. Ternier, K. Vyvey, and D. Cortina-Gil, *Phys. Rev. Lett.* **82**, 497 (1999).
- [5] N. Coulier, G. Neyens, S. Teughels, D.L. Balabanski, R. Coussement, G. Georgiev, S. Ternier, K. Vyvey, and W.F. Rogers, *Phys. Rev. C* **59**, 1935 (1999).
- [6] F. Hardeman, G. Scheveneels, G. Neyens, R. Nouwen, G. S'heeren, M. Van den Bergh, and R. Coussement, *Phys. Rev. C* **43**, 130 (1991).
- [7] K. Vyvey, G. Neyens, N. Coulier, R. Coussement, G. Georgiev, S. Ternier, S. Teughels, A. Lépine-Szilý, and D.L. Balabanski, *Phys. Rev. C* **62**, 034317 (2000).
- [8] F. Hardeman, G. Scheveneels, G. Neyens, R. Nouwen, G. S'heeren, M. Van den Bergh, and R. Coussement, *Phys. Rev. C* **43**, 514 (1991).
- [9] G. Neyens, R. Nouwen, G. S'heeren, M. Van Den Bergh, and R. Coussement, *Nucl. Phys.* **A555**, 629 (1993).
- [10] D.L. Balabanski, K. Vyvey, G. Neyens, N. Coulier, R. Coussement, G. Georgiev, A. Lépine-Szilý, S. Ternier, S. Teughels, M. Mineva, P.M. Walker, P. Blaha, D. Almeded, and S. Frauendorf, *Phys. Rev. Lett.* **86**, 604 (2001).
- [11] G. Neyens, S. Ternier, N. Coulier, K. Vyvey, R. Coussement, and D.L. Balabanski, *Nucl. Phys.* **A625**, 668 (1997).
- [12] R. Lutter, O. Häusser, D.J. Donahue, R.L. Hershberger, F. Riess, H. Bohn, T. Faestermann, F.v. Feilitzsch, and K.E.G. Löbner, *Nucl. Phys.* **A229**, 230 (1974).
- [13] O. Häusser, T.K. Alexander, J.R. Beene, E.D. Earle, A.B. McDonald, F.C. Khanna, and I.S. Towner, *Nucl. Phys.* **A273**, 253 (1976).
- [14] M. Ionescu-Bujor (private communication).
- [15] K. Vyvey *et al.*, *Phys. Lett. B* (to be published)
- [16] E. Matthias, W. Schneider, and R.M. Steffen, *Phys. Rev.* **125**, 261 (1962).
- [17] R. M. Steffen, and K. Alder, *The Electromagnetic Interaction in Nuclear Spectroscopy* (North-Holland, Amsterdam, 1975), p. 505.
- [18] H. Morinaga and T. Yamazaki, *In-beam Gamma-ray Spectroscopy* (North-Holland, Amsterdam, 1976).
- [19] U. Fano and G. Racah, *Irreducible Tensorial Sets* (Academic, New York, 1959).
- [20] G. Scheveneels, Ph.D. thesis, University of Leuven, 1988.
- [21] R. C. Weast, *Handbook of Chemistry and Physics* (The Chemical Rubber Company, Cleveland, Ohio, 1971).
- [22] R. B. Firestone, *Table of Isotopes*, 8th ed., edited by V. S. Shirley (Wiley, New York, 1996).
- [23] B. Fant, R.J. Tanner, P.A. Butler, A.N. James, G.D. Jones, R.J. Poynter, C.A. White, K.L. Ying, D.J.G. Love, J. Simpson, and K.A. Connell, *J. Phys. G* **17**, 319 (1991).
- [24] C. Stenzel, H. Grawe, H. Haas, H.-E. Mahnke, and K.H. Maier, *Z. Phys. A* **322**, 83 (1985).
- [25] J. Penninga, W.H.A. Hesselink, A. Balanda, A. Stolk, H. Verheul, J. van Klinken, H.J. Riezebos, and M.J.A. de Voigt, *Nucl. Phys.* **A471**, 535 (1987).
- [26] K. Vyvey, Ph. D. thesis, University of Leuven, 2001; P. Raghavan, *At. Data Nucl. Data Tables* **60**, 287 (1989), and references therein.
- [27] J.J. Van Ruyven, J. Penninga, W.H.A. Hesselinck, P. Van Nes, K. Allaart, E.J. Hengeveld, and H. Verheul, *Nucl. Phys.* **A449**, 579 (1986).
- [28] K. Vyvey *et al.*, *Phys. Rev. Lett.* (submitted).
- [29] S. Zywietz, H. Grawe, H. Haas, and M. Menningen, *Hyperfine Interact.* **9**, 109 (1981).
- [30] K.E.G. Löbner, M. Vetter, and V. Hönig, *Nucl. Data Tables* **7**, 495 (1970).
- [31] R. Bengtsson and W. Nazarewicz, *Z. Phys. A* **334**, 269 (1989).